

Magnetotransport in manganites and the role of quantal phases II: Experiment

S. H. Chun, M. B. Salamon, P. D. Han, Y. Lyanda-Geller, and P. M. Goldbart

Department of Physics and Materials Research Laboratory, University of Illinois at Urbana-Champaign, Urbana, Illinois 61801-3080

(April 22, 1999)

As in conventional ferromagnets, the Hall resistivity ρ_{xy} of a $\text{La}_{2/3}(\text{Ca,Pb})_{1/3}\text{MnO}_3$ single crystal exhibits both ordinary and anomalous contributions at low temperature. However, these contributions, unexpectedly, have opposite signs. Near T_c , the ordinary contribution is no longer evident and ρ_{xy} is solely determined by the sample magnetization, reaching an extremum at $\approx 40\%$ of the saturated magnetization. A new model for the anomalous Hall effect, incorporating the quantal phase accumulated by double-exchange, three-site hopping reproduces this result. Below T_c , ρ_{xy} reflects the competition between normal and anomalous Hall effects.

PACS No: 75.30.Vn, 72.20.My, 71.38.+i

Among the many intriguing properties exhibited by doped perovskite manganites, perhaps none is more puzzling than the Hall effect. A number of measurements have been reported on various members of the series $\text{La}_{1-x}\text{A}_x\text{MnO}_3$ (where A is Ca, Sr, or Pb), and all show common anomalous features [1–6]. At the lowest temperatures, the Hall resistivity ρ_{xy} is positive and linear in field, as expected for hole-doped materials, but rather smaller than expected. This has recently been attributed to charge compensation and Fermi-surface shape effects [6]. As the temperature is increased, a component of the Hall resistivity appears that is proportional to the magnetization $M(H, T)$, but has a negative sign. The appearance of an anomalous Hall effect is, of course, commonly observed in ferromagnets, but is usually attributed to spin-orbit scattering of the charge carriers and normally carries the same sign as the ordinary Hall contribution. A strong negative contribution to ρ_{xy} persists through the transition temperature, but loses its proportionality to M , until, at temperatures $\geq 1.5T_c$, ρ_{xy} becomes linear in field again (though negative) with a slope decreasing exponentially with increasing temperature in the manner expected for the Hall resistivity of small polarons [2,7,8]. Experimental data [6] suggest that charge transport is not polaronic in the temperature range $T_c - 1.5T_c$.

In this Letter, we present new Hall resistivity data on optimally doped manganite single crystals, with emphasis on the temperature region between the band-like, positive Hall regime at low temperatures and polaronic behavior at high temperatures. We show that the Hall resistivity ρ_{xy} is a function only of $M(H, T)$, reaching an extremum near $M/M_{\text{sat}} = 0.4$ when this value can be reached with laboratory fields at temperatures above the Curie temperature T_c . In fact, as we shall see, the data for all temperatures $T \geq T_c$ lie on a universal curve that follows from the theoretical model presented in a companion paper that we refer to as I [9]. Data taken below T_c track this universal curve once the magnetization is saturated, but are shifted to slightly larger values of $|\rho_{xy}|$. We argue that this is due to the return of band conduction as ferromagnetism, driven by double exchange, sets in.

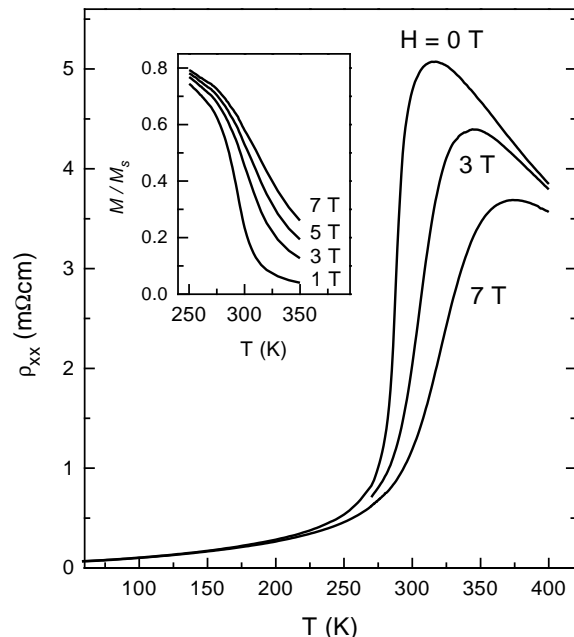


FIG. 1. Main panel: the temperature dependence of longitudinal resistivity $\rho_{xx}(H, T)$ of a $\text{La}_{2/3}(\text{Pb, Ca})_{1/3}\text{MnO}_3$ single crystal for different fields. Inset: the temperature dependence of magnetization $M(H, T)$ for the same crystal.

High quality single crystals of $\text{La}_{2/3}(\text{Ca,Pb})_{1/3}\text{MnO}_3$ were grown from 50/50 PbF_2/PbO flux. It was found that the addition of Ca favors optimally doped crystals; chemical analyses of crystals from the same batch gave the actual composition as $\text{La}_{0.66}(\text{Ca}_{0.33}\text{Pb}_{0.67})_{0.34}\text{MnO}_3$. Specimens for the Hall measurements were cut along crystalline axes from larger, pre-oriented crystals. Details of the measurement technique and analysis of the low temperature region have been presented elsewhere [6]. The Hall resistivity ρ_{xy} and longitudinal resistivity ρ_{xx} were measured simultaneously as functions of field and temperature. The magnetization of the same sample was measured following the Hall experiment, and was used to correct for demagnetization fields. Figure 1

shows the longitudinal resistivity as a function of temperature at zero field, 3 T and 7 T. Magnetization curves are shown in the inset. The residual resistivity of this sample, $\rho_{xx}^0 \approx 51 \mu\Omega \text{ cm}$, is comparable to the best values obtainable in these materials, indicating the absence of grain boundaries in our sample. The maximum change in resistivity with temperature $d\rho_{xx}/dT$ occurs at 287.5 K in zero field, moving to higher temperatures with increasing field. This gives rise to the ‘‘colossal magnetoresistance (CMR)’’ effect, which is 326% at 293 K and 7 T. A scaling analysis of the magnetization data very close to the metal-insulator transition (MIT) gives a Curie temperature of $T_c = 285 \text{ K}$, but this must be taken cautiously as the scaling exponents differ significantly from those expected from a 3D Heisenberg ferromagnet. Nevertheless, it is clear that ρ_{xx} and M are closely correlated in this system.

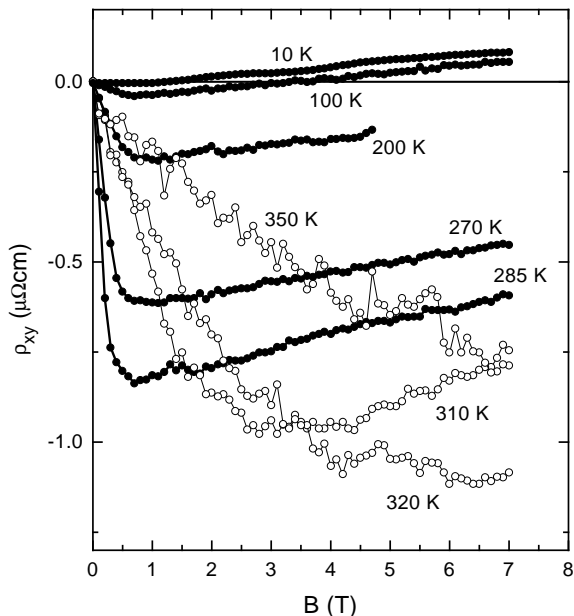


FIG. 2. Hall resistivity ρ_{xy} of the same crystal as a function of field at indicated temperatures.

In Fig. 2, we show the field dependence of ρ_{xy} at a number of temperatures. As noted above, the Hall resistivity is positive and linear in field at low temperatures, indicating that the anomalous Hall effect (AHE) is small. As the temperature is increased, the AHE contribution increasingly dominates the ordinary Hall effect (OHE), first causing ρ_{xy} to change sign as a function of field, and then driving it negative for all fields in the range measured. In ferromagnetic metals, the Hall resistivity is generally written as [10]

$$\rho_{xy} = R_H[\mu_0 H_{app} + \mu_0(1 - N)M] + R_S \mu_0 M, \quad (1)$$

where R_H is the coefficient of the OHE, while R_S is the coefficient of the anomalous contribution. In Fig. 2, we have plotted the data in terms of the internal field, given by the square brackets in Eq. (1), using a demagneti-

zation factor N calculated from the dimensions of the sample. As the temperature is increased through the transition temperature, the minimum of ρ_{xy} moves to higher fields, and the positive high-field contribution disappears. That there are rapid changes near T_c is not surprising because, even in an ordinary ferromagnet, R_S depends on longitudinal resistance which, in these samples, changes dramatically with temperature and applied field. However, R_S is then attributed to scattering from spin disorder, via either a skew-scattering [11] or side-jump processes [12], both of which require that the resistance be dominated by spin-disorder scattering. Even at low temperatures, where R_S is proportional to ρ_{xx} , the sign is opposite that expected from skew-scattering theory [11]. Further, as has been pointed out by many authors, the resistance changes observed here are too large to be the result of spin-dependent scattering, and must involve some form of localization, an effect we will invoke to explain the changes apparent here.

As discussed in I, we assume that transport in the transition region is dominated by hopping processes, giving rise to a longitudinal conductivity $\sigma_{xx} = (ne^2 d^2 / k_B T) W_0 \cos^2(\theta/2)$, where d is the distance between ions. Here W_0 is the probability of phonon-assisted direct hops and we have explicitly separated the Anderson-Hasegawa factors $\cos^2(\theta/2)$. The AH conductivity, correspondingly, is given by $\sigma_{xy} = (ne^2 d^2 / k_B T) W_1$, where W_1 is the probability of hopping between two ions via an intermediate state on a third ion and includes Anderson-Hasegawa factors [see Eq. (1) in I]. The problem then reduces to determining the ratio between direct and indirect hopping rates as a function of the spin texture. Because W_1 involves two-phonon processes, we write $W_1/W_0^2 = \alpha \hbar \zeta / k_B T$, where α is a numerical factor describing the multiplicity of the various carrier-phonon interference processes (see [8]), the number of intermediate sites, and the difference between nearest- and next-nearest-neighbor hopping amplitudes, and ζ is an asymmetry parameter. For the OHE, $\zeta \propto \sin(\mathbf{B} \cdot \mathbf{Q} / \phi_0)$, where \mathbf{Q} is the area vector of the triangle enclosed by the three sites. In the AHE case, it follows from Eqs.(2) and (4) in I that $\zeta \simeq 3[\mathbf{g}_{jk} \cdot (\mathbf{n}_j \times \mathbf{n}_k)][\mathbf{n}_1 \cdot (\mathbf{n}_2 \times \mathbf{n}_3)]/4$, where \mathbf{g}_{jk} are characteristic vectors arising from the spin-orbit quantal phase in the hopping amplitude; \mathbf{n}_j are unit vectors of the core spins in the triad, and $\mathbf{n}_1 \cdot (\mathbf{n}_2 \times \mathbf{n}_3)$ is the volume of a parallelepiped defined by core-spin vectors, denoted as q_P in I. The anomalous Hall resistivity can be written in the simple form

$$\rho_{xy} \simeq -\sigma_{xy}/\sigma_{xx}^2 = -\frac{1}{ne} \left(\frac{\alpha \hbar \zeta}{ed^2} \frac{1}{\cos^4(\theta/2)} \right). \quad (2)$$

The evaluation of Eq.(2) reduces to a determination of $\cos(\theta/2)$ and products $(\mathbf{n}_j \times \mathbf{n}_k)$ and $\mathbf{n}_1 \cdot (\mathbf{n}_2 \times \mathbf{n}_3)$ that survive averaging over all possible triads. In contrast to the hopping OHE in doped semiconductors [13], where only two sites in an optimal OHE triad are connected to the conducting network (CN), all three triad

sites must participate in the network if they are to contribute to the AHE. Our argument is that if one of the sites is not a part of the CN then its core spin must be roughly opposite that of the other two spins, yielding a vanishingly small q_P . It is reasonable then to assume that the CN is formed by ions with splayed core spins oriented roughly in the direction of average magnetization \mathbf{m} . We then consider the square lattice formed by Mn ions in planes perpendicular to \mathbf{m} , and assume that the core spin vectors of the four ions in a typical elementary plaquette belonging to CN lie equally spaced on the cone whose half angle is given by $\beta = \cos^{-1}[M(H, T)/M_{\text{sat}}]$. A typical pair of ions that determine the longitudinal current, and a typical triad can now be chosen from ions of this plaquette. From elementary geometry, it follows that $2 \cos^2(\theta/2) = 1 + \cos^2 \beta$, $q_P = 2 \cos \beta \sin^2 \beta$, and $\mathbf{m} \cdot (\mathbf{n}_j \times \mathbf{n}_k) = \sin^2 \beta$. To discuss the AHE magnitude, we need first to estimate the characteristic values of $|\mathbf{g}_{jk}| \sim g$ arising from the spin-orbit interaction (SOI). As we discussed in I, the SOI term leads to a Dzyaloshinski-Moriya contribution to the eigenenergy of carriers, whose magnitude is given by $g \sim Ze^2/4m_e c^2 d_0$, where d_0 is the radius of an Mn core d-state. An estimate based on free electron parameters gives $g \sim 5 \times 10^{-4}$. While renormalization of carrier parameters in crystals may tend to increase $|\mathbf{g}_{jk}|$, it is necessary to allow admixtures of core orbitals with outer-shell wavefunctions in order to have $|\mathbf{g}_{jk}| \neq 0$ for symmetric potentials. The non-collinearity of the Mn-O-Mn bonds that allows carrier hopping around triads (including jumps along plaquette diagonals) effectively generates such an admixture. Thus, a value of $g \sim 5 \times 10^{-4}$ is reasonable.

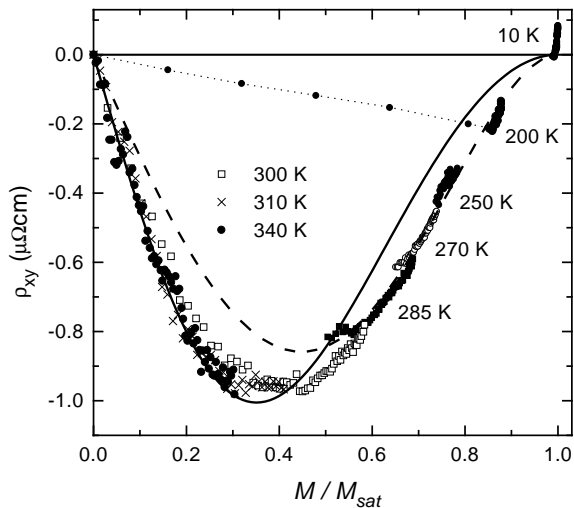


FIG. 3. Scaling behavior between ρ_{xy} and sample magnetization M . The solid line is a fit to Eq. (3); the dashed line is the numerator of Eq. (3) only. There are no fitting parameters except normalization.

As discussed in I, the magnitude of the longitudinal (and anomalous Hall) resistivities in the regime of abrupt increase of the resistivity depends not only on properties

of individual pairs (triads), but also on how are they connected to the CN. We estimate the macroscopic longitudinal and Hall conductivities at the low temperature limit of our model, where the CN is still fully connected. Taking $n = 5.6 \times 10^{21} \text{ cm}^{-3}$, $W_0 \sim 2.5 \times 10^{13} \text{ s}^{-1}$, and $\cos \beta = 0.6$ from the magnetization data at $T = 275 \text{ K}$ (Fig. 1), we obtain $\rho_{xx} \simeq 1 \text{ m}\Omega \text{ cm}$ which coincides with the value of the experimentally observed resistivity (Fig. 1). The AHE contribution to the Hall resistivity, assuming numerical factor $\alpha = 2.5$, is then $\rho_{xy} = -0.5 \text{ }\mu\Omega \text{ cm}$, in agreement with the experimentally observed Hall resistivity at the same T (Fig. 2). The equivalent expression for the hopping Hall resistance in the Holstein mechanism has $\zeta \simeq \cos^2(\theta/2) \cos \beta \sin(\mathbf{B} \cdot \mathbf{Q}/\phi_0)$ and, at $B = 1 \text{ T}$, is an order of magnitude smaller than the AHE. We expect the macroscopic, hopping AHE and OHE to have the same sign, opposite that of the OHE in the metallic regime.

To relate ρ_{xy} to $m \equiv |\mathbf{m}|$, we introduce a percolation factor P for σ_{xx} describing the connectivity of the pair to the CN; for the AH conductivity the corresponding factor would be P^2 because both pairs in a triad must, as discussed above, belong to the CN. It is remarkable that throughout the localization regime, ρ_{xy} is, nevertheless, determined by currents formed in individual pairs and triads, because the factors of P cancel. Therefore, as long as q_P and the angles between neighboring spins can be directly related to $m \equiv M/M_{\text{sat}} = \cos \beta$, ρ_{xy} depends on H and T only through $m(H, T)$, and is given by.

$$\rho_{xy} = \rho_{xy}^0 \frac{m(1 - m^2)^2}{(1 + m^2)^2} \quad (3)$$

The corresponding curve is shown in Fig. 3, where the data of Fig. 2 are replotted as a function of M/M_{sat} . At and above T_c the data fall on a smooth curve that reaches an extremum at $M/M_{\text{sat}} \simeq 0.4$. Below T_c the data first change rapidly with magnetization as domains are swept from the sample before saturating and following the general trend. At the lowest temperatures, the metallic OHE appears as a positive contribution at constant magnetization. The solid curve in Fig. 3 follows Eq. (3) with $\rho_{xy}^0 = -4.7 \text{ }\mu\Omega \text{ cm}$, consistent with the estimates of ρ_{xx} and ρ_{xy} given above. Down to 285 K, which is the Curie temperature determined by scaling analysis, Eq. (2) describes the data reasonably well. In addition, the extremum is located at $M/M_{\text{sat}} = \cos \beta \approx 0.35$, close to the experimental extremum. Below T_c , the longitudinal resistivity is metallic and no longer dominated by magnetic disorder. However, local spin arrangements still dominate the AHE via asymmetric scattering, as discussed in a forthcoming paper. The numerator of Eq.(3), $m(1 - m^2)^2$, essentially the behavior of σ_{xy} alone, has an extremum at $m = 1/\sqrt{5} \simeq 0.45$ as shown by the dashed line in Fig. 3. The broader maximum in the data suggest a shift toward a hopping model for ρ_{xx} and ρ_{xy} as the sample is warmed through the metal-insulator transition.

To consider the effect of OH contributions, which are

masked in ρ_{xy} by the large magnetoresistance, it is useful to examine the field and temperature dependence of σ_{xy} instead. As seen in the main panel of Fig. 4, the magnetic field dependence of σ_{xy} at 200 K clearly shows the OHE by free carriers at high fields, opposite in sign to the AHE. The AHE sign can be inferred by extrapolating the high field curve to its $B = 0$ intercept. At $T = 200$ K, ρ_{xx} is mainly metallic. At 265 K, where ρ_{xx} starts to increase rapidly, σ_{xy} saturates at external magnetic fields $H \sim 2$ T. At that magnetic field $M \sim 0.7M_{\text{sat}}$, relatively close to maximal value achievable at this temperature, $M \sim 0.8M_{\text{sat}}$ at 7 T. This saturation effect strongly suggests that the AHE is dominant and that the negative Holstein OHE [8] is either suppressed or partly compensated by the decrease in the AHE from reductions in qP by the magnetic field. As an increase in the magnetic field tends to delocalize carriers, we may expect to see the onset of metallic OHE at larger applied fields.

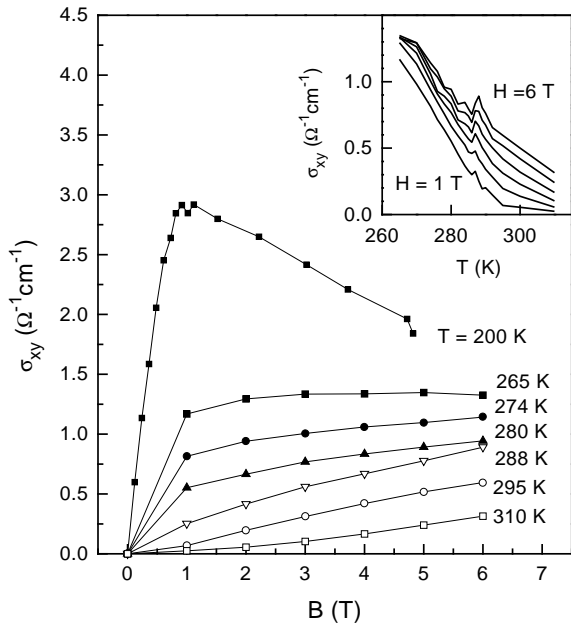


FIG. 4. Hall conductivity $\sigma_{xy}(H, T) = -\rho_{xy}/\rho_{xx}^2$ of the same crystal. Main panel shows the field dependence. The inset shows the temperature dependence for $H = 1, 2, 3, 4, 5, 6$ T from bottom to top.

Another interesting feature is that the temperature dependence of σ_{xy} shows an anomaly at the same temperature as the zero field $d\rho_{xx}/dT$ peak, (Fig. 4, inset). The size of the anomaly increases with increasing field, implicating the OHE. If this is related to a polaronic collapse of the conduction band [14], the anomaly should shift as H increases. However, peak shifts much less than does the $d\rho_{xx}/dT$ peak (see Fig. 1). To the extent that the transition is a percolation process in which metallic regions grow to form a percolation network, it is possible for the non-metallic Hall contribution to remain dominant down to the percolation threshold [15], resulting in the sudden

appearance of the OHE when the system becomes fully metallic. Indeed, this effect is evident, though less dramatic, in the Hall resistivity of Fig. 3, as a deviation of the data below T_c from the universal curve deduced from the quantal phase calculation.

In conclusion, we measured the Hall resistivity, the longitudinal resistivity, and the magnetization of a $\text{La}_{2/3}(\text{Ca,Pb})_{1/3}\text{MnO}_3$ single crystal. Very similar results have been observed in single crystals of Ca- and Sr-doped LaMnO_3 and will be reported elsewhere. We find that the Hall resistivity is solely determined by the sample magnetization (M) near and somewhat above the transition temperature. A model for the AHE, based on the Holstein picture in which interference between direct hops and those via a third site provides the necessary quantal phase [9], explains the results quite well. Unlike Holstein polarons, an additional phase here is introduced by the strong Hund's rule coupling that forces the hopping charge carrier to follow the local spin texture. Below the transition temperature, the AHE competes with the OHE as long-range magnetic order and, presumably, an infinite percolating metallic cluster, develops. A sharp, field dependent drop in the Hall conductivity at the transition temperature is qualitative evidence for this cross over between hopping-dominated Hall effects and features similar to those observed in more conventional ferromagnets.

This work was supported in part by DOE DEFG-91ER45439.

-
- [1] G. J. Snyder et al., *Appl. Phys. Lett.* **69**, 4254 (1996).
 - [2] M. Jaime et al., *Phys. Rev. Lett.* **78**, 951 (1997).
 - [3] P. Matl et al., *Phys. Rev. B* **57**, 10 248 (1998).
 - [4] G. Jacob et al., *Phys. Rev. B* **57**, 10 252 (1998).
 - [5] A. Asamitsu and Y. Tokura, *Phys. Rev. B* **58**, 47 (1998).
 - [6] S. H. Chun, M. B. Salamon, and P. D. Han, *Phys. Rev. B May* (1999).
 - [7] S. H. Chun et al. in preparation.
 - [8] T. Holstein, *Phys. Rev.* **124**, 1329 (1961); D. Emin and T. Holstein, *Ann. Phys. (N.Y.)* **53**, 439 (1969).
 - [9] Y. Lyanda-Geller, P. M. Goldbart, S. H. Chun, and M. B. Salamon, *Companion Letter I*, cond-mat/9904331.
 - [10] C. M. Hurd, *The Hall Effect in Metals and Alloys* (Plenum Press, New York, 1972).
 - [11] F. E. Maranzana, *Phys. Rev.* **160**, 421 (1967).
 - [12] L. Berger, *Phys. Rev. B* **2**, 4559 (1970).
 - [13] Y. M. Galperin et al., *Sov. Phys. JETP* **72**, 193 (1991).
 - [14] A. J. Millis, P. B. Littlewood, and B. I. Shraiman, *Phys. Rev. Lett.* **74**, 5144 (1995).
 - [15] D. J. Bergman and D. Stroud, in *Solid State Physics, Vol. 46*, edited by H. Ehrenreich and D. Turnbull (Academic Press, N.Y., 1992) p. 147.